Surface & Coatings Technology xxx (2015) xxx–xxx

Contents lists available at ScienceDirect

Surface & Coatings Technology

journal homepage: www.elsevier.com/locate/surfcoat

Nano-composite microstructure model for the classification of hydrogenated nanocrystalline silicon oxide thin films

Alexei Richter [a,*], Lei Zhao [b], Friedhelm Finger [a], Kaining Ding [a]

[a] IEK5-Photovoltaik, Forschungszentrum Jülich GmbH, 52425 Jülich, Germany
[b] Institute of Electrical Engineering, Chinese Academy of Sciences, Beijing 100190, China

ARTICLE INFO

Article history:
Received 13 May 2015
Revised 27 August 2015
Accepted in revised form 8 September 2015
Available online xxxx

Keywords:
PECVD
nc-SiOx:H
Hydrogenated nanocrystalline silicon oxide
Nano-composite
Optoelectronics
Thin-films

ABSTRACT

The unique microstructure of nanocrystalline silicon oxide (nc-SiO_X:H) thin films results in excellent optoelectronic properties that can be tuned in a wide range to fulfill the requirements of the specific application. For photovoltaic applications, this material is used as doped layers in silicon heterojunction solar cells and intermediate reflectors in multijunction thin-film solar cell. In this paper, we present a microstructure model based on a large number of n- and p-doped nc-SiO_X:H films that were deposited under various deposition pressures, plasma powers, plasma frequencies and gas mixtures. This model is meant to provide guidelines for the systematic classification of the complex material system nc-SiO_X:H by establishing a link between the structure of the deposited films and the optoelectronic performance of nc-SiO_X:H. Based on this model, the deposition of nc-SiO_X:H films can be divided into four characteristic regions: (i) fully amorphous region, (ii) onset of nc-Si formation, (iii) oxygen and nc-Si enrichment region, and (iv) deterioration of nc-Si. According to our microstructure model, an optimal phase composition with respect to the optoelectronic performance can be achieved with a high amount of highly conductive nc-Si percolation paths embedded in an oxygen rich a-SiO_X:H matrix.

1. Introduction

Hydrogenated nanocrystalline silicon oxide (nc-SiO_X:H) offers a unique combination of high transparency and conductivity. Thus, it has been researched extensively, especially for the application in silicon solar cells, e.g. as doped layers in silicon heterojunction solar cells [1–4] and wide gap window layers or intermediate reflectors in multijunction thin-film solar cells [5–7]. The excellent properties of nc-SiO_X:H films stem from their unique microstructure. That is, the combination of a highly conductive nanocrystalline silicon phase (nc-Si) and a superb transparency due to the amorphous silicon oxide (a-SiO_X:H) matrix. The individual contributions of these two phases provide a straightforward way to tune the optoelectronic properties of nc-SiO_X:H. However, during the PECVD deposition of nc-SiO_X:H many parameters like pressure, power, frequency and the individual gas flows can be varied, all of which affect the properties of the deposited thin films. Consequently, much research has been devoted to achieve the optimum trade-off between the conductivity and the optical properties of the material [5, 8–10] by tuning the deposition conditions. In this paper, we developed a microstructure model based on numerous n- and p-doped nc-SiO_X:H films that were deposited under various deposition pressures, plasma powers, plasma frequencies and gas mixtures to provide guidelines for a systematic classification of nc-SiO_X:H by establishing a link between the structure of the deposited films and the optoelectronic performance of nc-SiO_X:H. This classification helps to identify the structure of the deposited nc-SiO_X:H material and provides hints for further optimization steps.

2. Experimental

All nc-SiO_X:H thin films were deposited via plasma enhanced chemical vapor deposition (PECVD) on Corning glass substrates and polished mono-crystalline silicon at a substrate temperature of 200 °C. Silane (SiH_4), hydrogen (H_2) and carbon dioxide (CO_2) were used as precursors. All the while, n- and p-doping were achieved by additionally introducing phosphine PH_3 or trimethylborane $B(CH_3)_3$, respectively. Moreover, the nc-SiO_X:H was deposited at a plasma frequency of 81.4 MHz (VHF).

The sample thickness was determined using a commercial step profiling system (Vecco DEKTAK 6M Stylus Profiler). Structural characterization of the local bonding environments was performed by Fourier Transform Infrared Spectroscopy (FTIR) in a Nicolet 5700 FTIR. In addition, the oxygen content c_O of the samples was estimated from these FTIR spectra. In detail, the Si–O–Si stretching band was integrated from 950 cm^{-1} up to 1300 cm^{-1} using a correlation factor of $A(O) = 1.93 \cdot 10^{-5} \frac{at.\%}{cm^2}$ [11]. Another important structural parameter, the Raman crystalline intensity ratio I_C, was determined by a Raman Renishaw inVia Raman Microscope with a 532 nm Nd:YAG laser.

* Corresponding author.
E-mail address: ale.richter@fz-juelich.de (A. Richter).

http://dx.doi.org/10.1016/j.surfcoat.2015.09.016
0257-8972/

Hereby, I_C was defined as the ratio between the area of the crystalline Si peak at 520 cm^{-1} and the total peak area as reported by Lambertz et al. [12]. To characterize the optoelectronic performance of the films, the dark conductivity σ_D was measured with coplanar contacts and the spectral transmittance and reflectance of the films were obtained using a Perkin Elmer LAMBDA 950 spectrometer. The calculated spectral absorption coefficient $\alpha(\lambda)$ [13] was then used to identify the optical band gap E_{04} at $\alpha = 10^4$ cm^{-1}.

3. Results

The proposed microstructure model for PECVD grown nc-SiO_X:H thin films is based on numerous n- and p-doped films with thicknesses ranging from 100 nm to 1 μm. Two characteristic series of n-doped films were chosen to demonstrate the correlation between the deposition conditions, in particular the gas mixture, the microstructure of the films and their optoelectronic properties. In these series, the H_2 gas fraction f_{H2} was varied at two different CO_2 gas fractions f_{CO2}. The gas fractions were defined as:

$$f_{CO_2} = \frac{[CO_2]}{[CO_2] + [SiH_4]} \quad (1)$$

$$f_{H_2} = \frac{[H_2]}{[H_2] + [SiH_4] + [PH_3]} \quad (2)$$

where $[CO_2]$, $[SiH_4]$, $[H_2]$, and $[PH_3]$ are the gas flow rates of the corresponding gases.

Fig. 1 shows the Raman crystalline intensity ratio I_C, the dark conductivity σ_D, the oxygen content c_O, and the optical band gap E_{04} displayed versus f_{H2} for the aforementioned nc-SiO_X:H films. First of all, we consider the films deposited at a CO_2 fraction of 20% and divide them into four different deposition regions according to their material properties. At f_{H2} below 98.2%, the measured properties were independent of the amount of H_2 present in the gas phase. The oxygen content of these films was below 5 at.% and there was no c-Si peak at 520 cm^{-1} detectable in the Raman spectrum. The dark conductivity and optical band gap remained unchanged and showed typical values known from doped a-SiO_X:H films [14]. A f_{H2} beyond 98.2% led to films showing a crystalline peak in the Raman spectra as indicated by I_C. The dark conductivity increased as well. The total oxygen content of the films did not change, while the optical band gap was reduced. Starting from f_{H2} = 99%, the oxygen content and the optical band gap of the nc-SiO_X:H films increased with increasing H_2 (Fig. 1(c),(d)). At this point, the I_C had reached about 50% and σ_D started to decline with increasing f_{H2}. Beyond $f_{H2} \approx 99.5\%$, the conductivity then dropped significantly as the maximum in I_C was reached (Fig. 1(a),(b)). At the same time, the E_{04} strongly increased with rising f_{H2}.

Increasing the f_{CO2} from 20 to 40% resulted in a dependence of the material properties on f_{H2} similar to the f_{CO2} = 20% thin films. At the lowest f_{H2}, there was no crystalline peak present as indicated by the Raman crystallinity (Fig. 1(a)). However, the conductivity of this film was lower and the optical band gap was higher as compared to the films at f_{CO2} = 20%. Beyond 98.3% f_{H2}, the conductivity of the films drastically rose to similar values as for the nc-SiO_X:H deposited at f_{CO2} = 20%. Increasing f_{H2} over 99% then resulted in nc-SiO_X:H films with a steadily growing oxygen content and an increasing E_{04}. On the contrary, the σ_D declined, although the Raman crystallinity increased. Lastly, a f_{H2} larger than 99.5% resulted in a decay of I_C and a sharp drop in the conductivity. Unlike the f_{CO2} = 20% series, the oxygen content only marginally increased from 31 at.% on to 33 at.%. However, the steadily increasing optical band gap for larger f_{H2} is again comparable for both series.

Fig. 2 shows the sketched phase distribution of the films for the aforementioned f_{H2} deposition regions. Fig. 2(a)–(d) illustrates the microstructure consisting of three different phases, namely hydrogenated

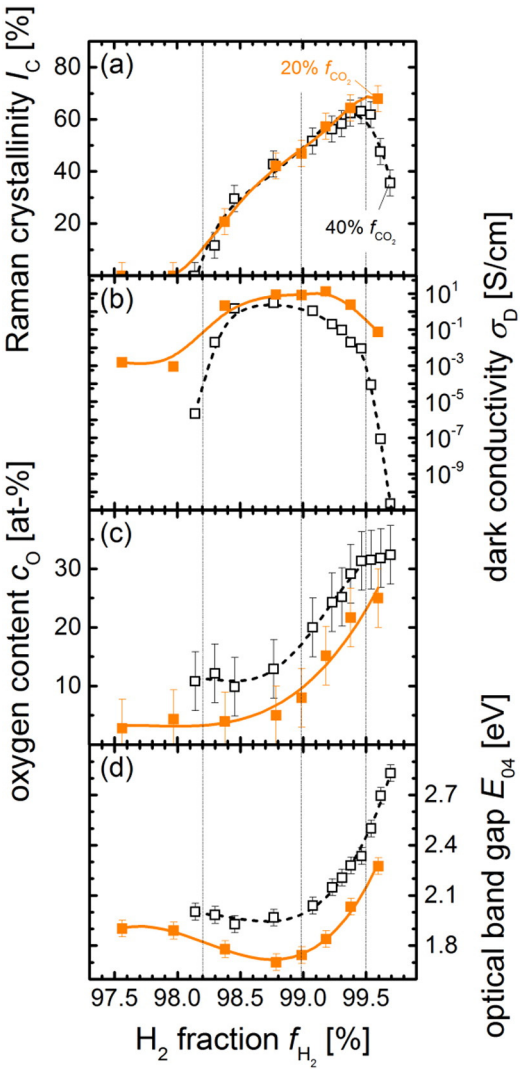

Fig. 1. (a) Raman crystallinity I_C, (b) lateral dark conductivity σ_D, (c) oxygen content c_O, and (d) optical band gap E_{04} of p-doped nc-SiO_X:H thin films for varying hydrogen fractions f_{H2}. The dashed vertical lines indicate four different regions of nc-SiO_X:H film deposition. The other lines are a guide to the eye.

amorphous silicon (a-Si:H), nanocrystalline silicon (nc-Si), and oxygen rich hydrogenated amorphous silicon oxide (a-SiO_X:H). Here, the a-SiO_X:H is assumed to have an oxygen content close to a-SiO_2 [7,15]. In Fig. 2(a), a-Si:H constitutes the main part of the microstructure with a low amount of a-SiO_X:H. In Fig. 2(b), nc-Si is now present and only small changes in the amount of the a-SiO_X:H phase occurred as compared to Fig 2(a). Fig. 2(c) shows that nc-Si takes over a significant part of the film volume and also a-SiO_X:H becomes present in large amounts. Finally, in Fig. 2(d), the microstructure is without any significant amounts of a-Si:H, while a-SiO_X:H and nc-Si dominate the microstructure. It is important to note that, in this sketch, the oxygen rich phase is partly disrupting percolation paths of the nc-Si.

Various exemplary IR spectra in the region of the Si–H stretching band from 1900 cm^{-1} to 2400 cm^{-1} are displayed in Fig. 3(a)–(d). These figures show the Si–H stretching peaks of selected nc-SiO_X:H films corresponding to different phase compositions in the microstructure. Four different peaks can be distinguished in these spectra. From high to low wavenumbers, these are approximately located at 2250 cm^{-1}, 2190 cm^{-1}, 2100 cm^{-1}, and 2000 cm^{-1}. In Fig. 3(a) for the f_{CO2} = 20% sample, the peak at 2100 cm^{-1} dominates the spectrum with a significant shoulder at 2000 cm^{-1} and two shoulders towards higher wavenumbers. For the f_{CO2} = 40% nc-SiO_X:H film, the peak at

Please cite this article as: A. Richter, et al., Nano-composite microstructure model for the classification of hydrogenated nanocrystalline silicon oxide thin films, Surf. Coat. Technol. (2015), http://dx.doi.org/10.1016/j.surfcoat.2015.09.016